Reinforced cast glass

Embedded metal reinforcement for resilient and circular structural cast glass components

Oikonomopoulou, F.; Ioannidis, M.; Bristogianni, T.

DOI
10.1201/9781003677895-144

Publication date
2025

Document Version
Final published version

Published in
Engineering Materials, Structures, Systems and Methods for a More Sustainable Future

Citation (APA)
Oikonomopoulou, F., Ioannidis, M., & Bristogianni, T. (2025). Reinforced cast glass: Embedded metal reinforcement for resilient and circular structural cast glass components. In A. Zingoni (Ed.), *Engineering Materials, Structures, Systems and Methods for a More Sustainable Future* (pp. 863-868). CRC Press / Balkema - Taylor & Francis Group. https://doi.org/10.1201/9781003677895-144

Engineering Materials, Structures, Systems and Methods for a More Sustainable Future – Zingoni (Ed.)
© 2025 The Author(s), ISBN 978-1-041-15001-5

Reinforced cast glass: Embedded metal reinforcement for resilient and circular structural cast glass components

F. Oikonomopoulou, M. Ioannidis & T. Bristogianni
Faculty of Architecture, Department of Architectural Engineering + Technology, TU Delft, Delft, The Netherlands

ABSTRACT: Glass casting offers the potential to create complex, large-scale, monolithic structural elements with optimized stiffness and material use. However, glass's brittleness and lack of post-failure redundancy pose safety challenges, especially since conventional float glass safety strategies are difficult to apply to volumetric components. Inspired by reinforced concrete, this study explores embedding metal reinforcement in cast glass directly during the casting process to enhance ductility, redundancy, and recyclability by avoiding adhesives. The novelty lies in directly bonding metal to glass using materials with similar thermal expansion coefficients, further allowing contamination-free recycling. Building on previous TU Delft research, we investigate two material combinations with matching thermal expansion coefficients: (i) borosilicate glass with F15 Kovar and (ii) soda-lime silica glass with Titanium Grade 2 or 5. Kiln-cast glass beams with a longitudinal metal reinforcement are produced and tested under four-point bending using Digital Image Correlation to assess their mechanical performance. Borosilicate glass specimens reinforced with Kovar demonstrated effective glass-metal interaction but lower strength due to interfacial bubbles, with all specimens failing in shear, in a similar manner to reinforced concrete, while retaining most glass attached to the metal rod. Soda-lime glass specimens reinforced with Titanium exhibited higher failure loads, though specimens reinforced with Grade 2 Titanium failed in bending similar to unreinforced glass. Titanium Grade 5 reinforcement showed potential for strength enhancement and progressive failure, emphasizing the importance of proper reinforcement selection and dimensioning. Finally, we discuss the potential for material separation at end-of-life and the applicability of this technology for embedded connections in cast glass.

1 INTRODUCTION

Glass casting is a promising manufacturing method capable of producing structural glass components in virtually any shape and size, as demonstrated from intricate glass art pieces to massive monolithic telescope mirrors. In architecture, current research at TU Delft on the use of topology optimization (TO) and associated fabrication methods exhibits the possibilities of casting large-scale monolithic, customized structural glass elements, such as beams and bridges (Figure 1), which can maintain structural integrity with optimal stiffness and material use (Damen *et al.* 2022; Ioannidis *et al.* 2024; Koniari *et al.* 2023; Oikonomopoulou *et al.* 2022; Oikonomopoulou *et al.* 2023). A remaining challenge for unlocking the real-world applicability of such monolithic cast glass structures in the built environment, is their lack of any post-breakage redundancy. Due to its brittle nature, glass will fail suddenly and without warning, making it difficult to ensure structural safety after failure. Common structural safety strategies applied to float glass, such as tempering, chemical strengthening and lamination, are challenging to implement in volumetric glass (Bristogianni and Oikonomopoulou 2022a).

Concrete, a widely used material for structural applications, demonstrates a similar structural behavior to glass: it is a durable yet brittle, with a compressive strength of at least a magnitude higher than its tensile strength. To prevent a brittle, sudden failure, concrete structural members are typically reinforced with steel bars. The latter further serve to resist tensile forces, distribute cracks, and control crack width.

Figure 1. Illustration of a monolithic, topology optimized cast glass cantilever by M. Ioannidis.

Adhesively-bonded metal reinforcement in laminated float beams has been experimentally investigated in (Belis *et al.* 2009; Cupać *et al.* 2021; Louter 2011; Nielsen and Olesen 2007; Veer *et al.* 2003). The hybrid glass components achieve a ductile behavior

DOI: 10.1201/9781003677895-144

upon failure and show significant post-breakage redundancy, as the fractured pieces remain connected.

In previous work (Bristogianni and Oikonomopoulou 2022a) the authors have demonstrated that incorporating metal reinforcement in cast glass directly during casting enables strong composite action, similar to reinforced concrete. Moreover, the direct bond between the two materials can enhance recyclability, allowing for easy material separation. To avoid thermal stress cracking it is essential that the chosen glass and metal have nearly identical thermal expansion coefficients. Existing applications, e.g. wired safety glass, glass-to- metal seals for electronics, demonstrate the feasibility of this approach.

In this paper, we build upon our previous work on reinforced cast glass beams, by kiln-casting and mechanically testing under 4-point bending series of glass beams of 30x30x240mm in size, with two promising combinations of glass and metal: (i) Borosilicate glass with F15 Kovar and (ii) Soda-lime silica (float) glass with Titanium Grade 2 and Grade 5. We also reflect on the potential separation of the two materials at the end-of-life and of using this direct metal-to-glass bond for embedded connections in cast glass.

2 EXPERIMENTAL

2.1 *Kiln-casting of specimens*

Based on the findings of Bristogianni and Oikonomopoulou (2022a), two combinations of glass and metal are used for the kiln-casting of 30×30×240 mm beams with longitudinal metal reinforcement in the form of a rod. These are: (i) Alkali Borosilicate (7056 Corning) glass with ø 4mm or ø 6mm F15 Kovar rod; (ii) Soda-lime silica (float) glass with ø 4mm Titanium Grade 2, or a ø 4mm or ø 6mm Grade 5 rod. All beams are kiln-cast in silica plaster investment moulds (Crystalcast M248). The metal bar is placed along the length of the beam at the bottom of the mould and covered with glass in cullet form (Figure 2). The beams are then kiln-cast in a *ROHDE ELS 1000S* kiln employing the firing schedules

Table 1. Material combination, thermal exp. Coefficient (α) and firing schedule temperatures.

Glass			Metal			Temp. ** °C	
Type	Composition	α*	Type	Composition	α*	Form	Anneal
Alkali Borosilicate	68% SiO_2 18% B_2O_3 11% alkali oxides	5.15	F15 Kovar	54% Fe 29% Ni 17% Co	5.2	870	512
Soda lime silica	75% SiO_2 12% Na_2O 8% CaO	8.7	Gr2 Ti Gr5 Ti	99% Ti 90% Ti 6% Al 4% V	9.2 9.2	1120	560

*Thermal expansion coefficient in 10^{-6} K^{-1}, reported in the literature for a 20-300°C range.
**Dwell time 10h both at forming and annealing temperature.

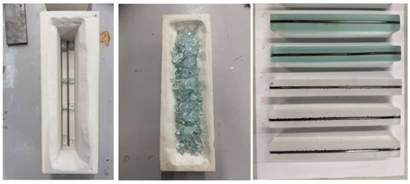

Figure 2. From left to right: Placement of the reinforcement at the bottom of the mould; filling the mould with glass cullet; glass beams after being cast and manually polished to 600 grit.

identified as the most promising in our previous work (Table 1). The beams are then manually polished up to 600 grit (Figure 2) and visually inspected for cracks and other defects.

2.2 *4-point bending tests*

An overview of the specimens can be found in Table 2 at the Results section. Before testing, the polished beams are sprayed with a white-black speckle pattern to enable displacement measurement using Digital Image Correlation (DIC). The specimens are tested under 4-point bending until failure using a UTM-25 Universal Testing Machine at a displacement rate of 0.01 mm/s. During testing, high-res pictures are taken at a rate of 1 picture per 2 seconds, to be later analyzed with the aid of GOM Correlate software. The setup includes a 100 mm loading span with ø14 mm pin rollers and 200 mm support span with ø20 mm fixed rollers. A neoprene interlayer is placed between the glass beam and the steel supports, to prevent peak stresses generating from the direct contact of the two materials. The set-up is shown in Figure 3. To verify the setup and displacement rate, a calibration test is first performed using a 12 mm thick waterjet cut float glass dummy specimen under the same conditions.

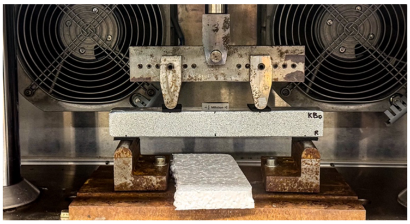

Figure 3. Four-point bending test set-up of specimen $BK_6 1$.

3 RESULTS

3.1 *Visual inspection of kiln-cast specimens*

Visual inspection on the kiln-cast specimens revealed a good interface quality between the Titanium bars and the soda-lime glass. In contrast, all Kovar-Borosilicate specimens presented significant bubble formation near the metal reinforcement, which could potentially act as weaking points (Figure 4). The bubbles can be minimized if the specimens are cast in a slightly higher temperature. A check of the specimens under cross-polarized light did not reveal major residual stresses at the glass-to-metal interface.

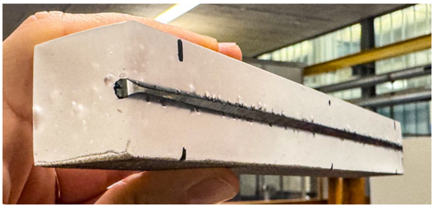

Figure 4. Visible bubbles along the metal reinforcement-glass interface at the Kovar-Borosilicate specimens.

Table 2 provides a summary of the 4-point bending results and Figure 5 provides the corresponding force-displacement chart. The following labeling approach is used for the specimens:

$$WXyZ$$

where,

- W indicates the type of glass (**B** = borosilicate, **S**=soda-lime);
- X shows the type of metal reinforcement (**Ti2**=Titanium Gr2, **Ti5**=Titanium Gr5, **K**= Kovar);
- y shows the reinforcement diameter in mm;
- Z is the number of the specimen.

For example, $STi2_43$ is specimen number 3 made of soda-lime glass reinforced with ø 4mm Ti Gr2 bar.

Table 2. Overview of tested glass beam specimens.

Specimen	w [mm]	h [mm]	Force at first crack [N]	Force at failure [N]	Flex. strength [MPa]	Failure mode
Float	30	12	-	1119	38.9	bending
BK_61	29.8	30.5	2293	6857	37.1	shear
BK_41	30	31.5	2274	4624	23.3	shear
BK_42	30	30.9	2306	4337	22.7	shear
BK_43	29.9	31.3	2606	5434	28.0	shear
$STi2_41$	28.8	28.9	-	7906	49.3	bending
$STi2_42$	29.6	30.5	-	8728	47.7	bending
$STi2_43$	28.8	29.6	-	8245	49.1	bending
$STi5_41$	28.8	29.4	-	9011	54.3	bending
$STi5_61$	29.0	29.9		9347	54.0	shear

3.2 *Kovar reinforced Borosilicate (BK) specimens*

All Borosilicate-Kovar (BK) beams began cracking at significantly lower loads (~2.2–2.6 kN) compared to the Soda-Lime-Titanium (STi) series. This is attributed to the presence of multiple bubbles at the glass-metal interface of the BK beams that could potentially compromise their strength. All BK specimens exhibited shear failure due to diagonal cracks formed at the zones between the support and loading rollers, following the progressive development of vertical tensile cracks within the maximum stress zone (Figure 6). These tension-induced cracks were arrested towards the compression zone of the glass beams, as illustrated in the processed DIC images in Figure 6 and in alignment with our previous findings at (Bristogianni, Oikonomopoulou 2022a).

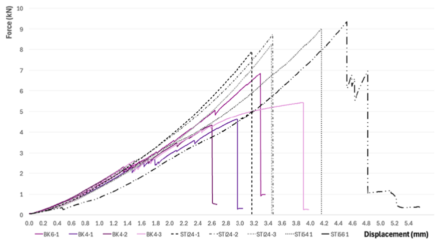

Figure 5. Force-displacement chart for all specimens.

BK_41-3 specimens, all reinforced with a ø4mm Kovar rod, failed at a flexural strength of 22.7–28 MPa. In contrast, specimen BK_61, which has ø6mm reinforcement, despite cracking at a similar load as BK_41-3 beams, failed at a much higher strength (37.1 MPa). This suggests effective interaction between the glass and metal reinforcement after cracking, with tensile forces primarily carried by the reinforcement.

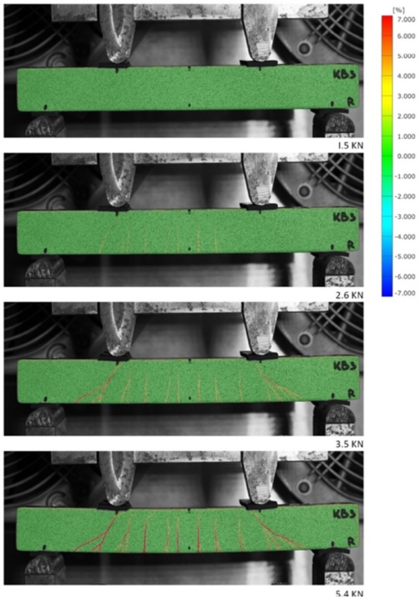

Figure 6. Major strain in BK_43 beam specimen shown under 1.5 kN, 2.6 kN, 3.5kN and 5.4kN loading. First, vertical tension cracks appear, followed by diagonal shear cracks that eventually lead to failure. The vertical cracks are arrested towards the top, compression zone of the beam.

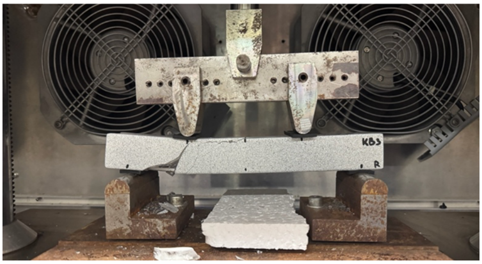

Figure 7. Shear failure of specimen BK_43.

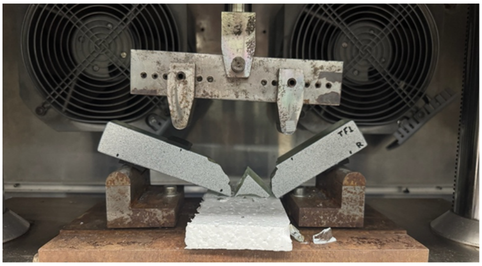

Figure 8. Bending failure mode of specimen $STi2_41$.

The force-displacement graph (Figure 5) indicates that the tested beams follow a three-stage failure mechanism - elastic, cracked, and yield - with distinct stiffness changes at each stage, similar to the one observed by Nielsen and Olesen (2007) at laminated, steel-reinforced glass beams. In the yield phase, some ductile behavior is evident before failure in the BK_41-3 specimens, which have less reinforcement than the BK_61specimen. The observed shear failure through diagonal cracking is typical in higher reinforced concrete beams without transverse reinforcement (Słowik 2018), similar to the reinforcement setup used here.

After failure, the metal bar remains intact, with most of the glass mass still attached to it, while some glass fragments shatter (Figure 7). This suggests a degree of post-failure load-bearing capacity.

3.3 *Titanium reinforced Soda-lime (STi) specimens*

All beams reinforced with ∅ 4mm Titanium Gr2 rod ($STi2_41$ – $STi2_43$) failed under bending, at considerably higher loads and without visible cracking prior to failure. In all 3 specimens, the Ti reinforcement snapped upon failure and the specimens split in half by a flexural crack, as if no reinforcement was present (Figure 8). A very rough calculation indicates that at the failure load, the stress in the Ti Gr2 bar was indeed higher than its ultimate tensile strength. In specific, the specimens failed in bending at 47.7–49.3 MPa, exhibiting a failure stress comparable to the mean failure stress (47.7MPa) of pure soda-lime glass beams of identical composition and dimensions tested under the same 4-point bending setup (Bristogianni, Oikonomopoulou 2022b). Both the failure mode and failure load suggest that in this case, the metal reinforcement was inadequate to guarantee a collaboration with the glass and to carry the excessive tensile stresses. Specimen $STi5_41$, reinforced with ø 4mm Titanium Gr5 rod failed at a similar manner, yet at a slightly higher failure load (54 MPa). This may suggest a degree of collaboration between the reinforcement and the glass, although further testing is necessary to confirm this.

In contrast, specimen $STi5_61$, reinforced with a ø 6mm Titanium Gr5 rod failed at 54 MPa in shear, in a similar manner to the BK specimens; initially arresting vertical cracks in the tensile zone of the specimen appeared, followed by diagonal cracking at the zone between the support and loading rollers; after breaking, most of the glass remained attached to the rod.

4 CONCLUSION

This research focuses on a novel reinforcement method for cast glass that prevents its sudden failure, allowing instead for relatively ductile failure and progressive cracking, through the direct bond of metal to glass with compatible thermal expansion coefficient. Two material combinations are explored via kiln-casting prototypes and 4-point bending experiments employing DIC:

i) Alkali Borosilicate (7056 Corning) glass reinforced with a F15 Kovar bar;
ii) Soda-lime silica (float) glass reinforced with Titanium Grade 2 or Grade 5 bar.

Figure 9. Shear failure of BK series (left) vs the brittle flexural failure of STi2 series (right).

The Borosilicate-Kovar (BK) beams cracked at lower loads than the Soda-lime-Titanium (STi) ones, due to multiple bubbles at the glass-metal interface, which weakened the specimens. The forming temperature should be further adjusted to prevent the occurrence of large bubbles and thus, increase the strength.

All BK specimens showed an effective interaction between the glass and metal reinforcement; the beams failed under shear after progressive, visible cracking at considerably lower loads in a similar manner to reinforced concrete without transverse reinforcement. After failure, the metal bar remained intact, with glass fragments attached, indicating some post-failure load-bearing capacity (Figures 7 and 9).

The force-displacement graph showed a three-stage failure process -elastic, cracked, and yield- similar to laminated, steel-reinforced glass beams. Beams with less reinforcement (∅4mm) failed at lower stress values (22.7–28 MPa) than the specimen with higher reinforcement (∅6mm, failed at 37.1 MPa), suggesting reinforcement effectiveness.

In comparison, the soda-lime glass beams reinforced with Titanium Gr2 rods ($STi2_41$-3), failed at significantly higher loads (47.7–49.3 MPa), due to bending (Figures 8 and 9) and without any prior visible cracking. Upon failure, the Titanium reinforcement snapped, providing no structural benefit. The failure load matched previous tests on pure soda-lime glass beams, further indicating that the Titanium reinforcement was insufficient to effectively carry tensile stresses; yet, it also did not lead to a compromise in the strength of the beams.

Both soda-lime glass specimens reinforced with Titanium Gr5 rods ($STi5_41$ and $STi5_61$) failed at a load circa 10% higher than the $STi2_41$-3 specimens reinforced with Titanium Gr2 and the previously tested pure soda-lime glass beams, suggesting that the reinforcement may be able to not only provide a safer failure mode for the hybrid glass beams, but possibly increase their strength as well.

Specimen $STi5_61$, which was reinforced with a ∅6mm Titanium Gr5 rod, failed under shear, in a similar manner as the BK specimens. This result confirms that effective interaction between the soda-lime glass and Titanium reinforcement is possible, and proper dimensioning of the latter is important for ensuring its effectiveness.

At the end of the hybrid component's life, the direct bond allows for the eventual mechanical separation of the glass and metal components, enabling the recyclability of both materials. A simple experiment with a magnet on the broken BK specimens, confirms that Kovar can be magnetically removed, further facilitating the separation and recyclability of the two materials (Figure 10). Overall, the disassembly process is simpler than the labour-intensive separation of laminated or adhesively-bonded reinforcements, which bear contamination from adhesives.

Figure 10. Magnetizing the Kovar rod after the hybrid glass beam is cast.

The direct adhesion of glass and metal via casting opens new possibilities for direct embedded connections in cast glass, with further applicability also to 3D printed glass. The casting-based direct adhesion of glass and metal, which facilitates mechanical separation and recyclability, makes it a particularly promising solution for embedded connections or reinforcement in recycled cast (or 3D printed) glass components, enabling a full circular approach at the end-of-life.

5 RECOMMENDATIONS

The findings indicate that direct metal-to-glass bonding is feasible when materials with nearly identical thermal expansion coefficients are used, offering a promising solution to evade the brittle, sudden failure of monolithic, large-scale cast glass structural elements while maintaining, or possibly even increasing, their strength. Further testing is required to validate this observation, as the experiments presented in this study, while promising, are limited in scope and sample size to draw definitive conclusions.

Further research can focus on finite element analysis (FEA) using the experimental results to optimize reinforcement arrangements and profiles, towards improving the bond strength and the load distribution between glass and metal, and the ductility of the hybrid beams.

ACKNOWLEDGEMENTS

The authors would like to thank Giorgos Stamoulis

(TU Delft) and Wilfried Damen for their valuable assistance with the experimental work, and Dr. Michel Prassas (Corning France) for providing the borosilicate glass cullet.

REFERENCES

Belis, J., Callewaert, D., Delince, D. and Van Impe, R. (2009). Experimental failure investigation of a hybrid glass/steel beam. *Engineering Failure Analysis 16*(*4*), p. 1163–1173.

Bristogianni, T. and Oikonomopoulou, F. (2022a) Reinforced glass: structural potential of cast glass beams with embedded metal reinforcement. *Eighth*

International Conference on Structural Engineering, Mechanics and Computation (SEMC), Cape Town, A. Zingoni, Ed., Taylor & Francis.

Bristogianni, T. and Oikonomopoulou, F. (2022b) Glass Up-casting: a review on the current challenges in glass recycling and a novel approach for recycling "as-is" glass waste into volumetric glass components. *Glass Structures and Engineering 8*, *p.*255–302.

Cupac, J., Louter, C. and Nussbaumer, A. (2021) Flexural behaviour of post-tensioned glass beams: Experimental and analytical study of three beam typologies. *Composite Structures 255*.

Damen, W., Oikonomopoulou, F., Bristogianni, T. and Turrin, M. (2022) Topologically optimized cast glass: a new design approach for loadbearing monolithic glass components of reduced annealing time. *Glass Structures & Engineering*, vol. 7, pp. 267–291.

Ioannidis, M., Oikonomopoulou, F., Bristogianni, T., Bilow, M. and Koniari, A.M. (2024) Surface and finishing quality exploration of complex cast glass forms produced on disposable moulds. *Glass Structures and Engineering*, Vol. 9, p. 357–381.

Koniari, A., Andriotis, C. and Oikonomopoulou, F. (2023) Minimum mass cast glass structures under performance and manufacturability constraints. *CAAD Futures 2023*, Delft.

Louter, P.C. (2011). *Fragile yet Ductile: Structural Aspects of Reinforced Glass Beams*. Delft University of Technology.

Nielsen, J.H. and Olesen, J.F. (2007). Mechanically reinforced glass beams.: *The Third International Conference on Structural Engineering, Mechanics and Computation*, Cape Town, South Africa. Millpress.

Oikonomopoulou, F., Ioannidis, T., Koniari, A.M. and Bristogianni, T. (2023). Fabrication Methods for topology-optimized massive glass structures. *Proceedings of the IASS Annual Symposium 2023 Integration of Design and Fabrication*, Melbourne.

Oikonomopoulou, F., Koniari, A., M., Damen, W., Koopman, D., Stefanaki, I., M.and Bristogianni, T. (2022). Topologically optimized structural glass megaliths: Potential, challenges and guidelines for stretching the mass limits of structural cast glass. *Eighth International Conference on Structural Engineering, Mechanics and Computation (SEMC)*, Cape Town, A. Zingoni, Ed., Taylor & Francis.

Slowik, M. (2018). The analysis of failure in concrete and reinforced concrete beams with different reinforcement ratio. *Achive of Applied Mechanics*.

Veer, F.A., Gross, S., Hobbelman, G.J., Vredeling, M., Janssen, M.J.H.C., Van der berg, R. and Rijgersberg, H.A. (2003). Spanning structures in glass. *Glass Processing Days*, Tampere, Finland.